

Modelling and FEA-simulation of the anisotropic damping of thermoplastic composites

Matthias Klaerner^{*1}, Mario Wuehrl^{1a}, Lothar Kroll^{1b} and Steffen Marburg^{2c}

¹*Institute of Lightweight Structures Technische Universität Chemnitz, 09107 Chemnitz, Germany*

²*Lehrstuhl für Akustik mobiler Systeme, Technische Universität München, 85748 Garching, Germany*

(Received June 14, 2015, Revised August 11, 2015, Accepted August 19, 2015)

Abstract. Stiff and light fibre reinforced composites as used in air- and space-craft applications tend to high sound emission. Therefore, the damping properties are essential for the entire structural and acoustic engineering. Viscous damping is an established and reasonably linear model of the dissipation behaviour. Commonly, it is assumed to be isotropic and constant over all modes. For anisotropic materials it depends on the fibre orientation as well as the elastic and thermal material properties. To portray the orthogonal anisotropic behaviour, a model for unidirectional fibre reinforced plastics (frp) has been developed based on the classical laminate theory by ADAMS and BACON starting in 1973. Their approach includes three damping coefficients - for longitudinal damping in fibre direction, damping transversal to the fibres and shear based dissipation. The damping of a laminate is then accumulated layer wise including the anisotropic stiffness. So far, the model has been applied mainly to thermoset matrix materials. In this study, an experimental parameter estimation for different thermoplastic frp with angle ply and cross ply layups was carried out by measuring free vibrations of cantilever beams. The results show potential and limits of the ADAMS/BACON damping criterion. In addition, a possibility of modelling the anisotropic damping is shown. The implementation in standard FEA software is used to study the influence of boundary conditions on the damping properties and numerically estimate the radiated sound power of thin-walled frp parts.

Keywords: damping; thermoplastic composites; FEA simulation; anisotropy

1. Introduction

Lightweight structures in air- and space-craft applications with high stiffness and low density tend to be sensitive to vibrations and thus to structure borne sound radiation. Such fibre reinforced plastics (frp) offer a unique range of adjustable material properties by numerous influencing parameters such as fibre and matrix material, fibre volume content, textile structure of fabrics, fibre orientation and layup. The linear elastic anisotropic behaviour of the lamina is reasonably estimated based on the orthogonal material properties of the single layers by the classical laminate theory (CLT). Moreover, different phenomenological and physically based failure criteria are used

*Corresponding author, Ph.D. Candidate, E-mail: matthias.klaerner@mb.tu-chemnitz.de

^aStudent, E-mail: mario.wuehrl@mb.tu-chemnitz.de

^bProfessor, E-mail: lothar.kroll@mb.tu-chemnitz.de

^cProfessor, E-mail: steffen.marburg@mw.tum.de

to describe the different strength properties.

In contrast, damping prediction of frp by basic assumptions as the rule of mixture or micro mechanics is not suitable due to the missing fibre-matrix interactions. Thus, damping in orthotropic materials can not be described as material property, only. It needs to be treated as a complex relation of the orthogonal material properties, the layup and the modal deformation characteristics including all boundary conditions (Maheri 2011).

A well-known model for the damping prediction of laminated plates with anisotropic behaviour both in stiffness and damping has been introduced by ADAMS & BACON (Adams *et al.* 1973). Developed for beams first, the ADAMS-BACON model (ABM) has been successfully tested for several thermoset based composites (Ni *et al.* 1984). A summary of different investigated composites in literature regarding the static material properties for the lamina is given in Table 1. Therein, E and G are respectively tensile and shear modulus, ν Poisson ratio, ν_f the fibre volume fraction as well as ψ the damping coefficients in the principal material directions of a lamina (1, 2).

First assumptions allowed stress dependency of the coefficients being later neglected due to easier solutions. The model has been improved by taking into account bending-twisting coupling for free flexure, too (Ni *et al.* 1984). Still, the transverse strain was neglected being much smaller than the longitudinal and shear strains but later introduced by Adams *et al.* (1994).

Further investigations showed no significant effect of beam width and, thus, proved the applicability for the model (Ni *et al.* 1984). Frequency dependency of polymer material behaviour can be assumed to be constant in a limited frequency range.

Strictly, the damping properties of frp depend on the stress amplitudes but may be considered constant for small vibration amplitudes (limited to 10-20% of the ultimate strength) (Lin *et al.* 1984). In contrast, amplitude dependency was mentioned only for the shear related SDC ψ_{12} of some composites. Thereby, none of the other moduli or damping coefficients was significantly stress dependent (Adams *et al.* 1973).

In addition, effects of moisture and temperature on the shear loss factor of epoxy and PEEK based frp are shown in Adams *et al.* (1996) as well as a wide range of temperature effects on different frp (Maheri *et al.* 1996).

Further on, the model has been extended to two-dimensional cases. Good predictions for plates are based on the finite element analysis or on the Rayleigh-Ritz method (Adams *et al.* 2003, Maheri *et al.* 2003). A general overview of corresponding models can be found in Chandra *et al.* (1999) and is not explained in detail here.

The ABM has been used recently for several investigations on frp damping behaviour. Parametric studies including the layup and boundary conditions have shown the design possibilities of the modal damping of frp (Maheri 2011). Further studies include the influence of material and layup on the damping (Täger *et al.* 2004) and, thus, the radiated sound of plates (Täger *et al.* 2015) including results of Polypropylene and Polyamide based frp.

The model has been further applied for sandwich structures with different cores and frp face sheets (Maheri *et al.* 2008, Hazrati 2013). The influence of the fibre-matrix interface has been proved using the ABM and different fibre diameters of glass fibre reinforced plastics (Nagasankar *et al.* 2014). A further increase of damping can be achieved by interleaving visco-elastic layers (Yim *et al.* 2003, Kishi *et al.* 2004). Additional works on composite damping properties and models have been chronologically reviewed by Trev *et al.* (2015).

In summary, anisotropic damping of composite structures is state of the art for thermoset based frp and usually based on three plane stress related damping constants for a unidirectional

reinforced plastic material. The applicability of the models is focused on thermoset matrix materials so far.

Thermoplastic frp offer less shear stiffness within the matrix material and tend to show matrix accumulations between the fibre layers depending on their impregnation technology (e.g., film stacking). This may encourage interlaminar shear deformations especially for angle ply layups which is in contrast to the basic assumptions of CLT and ABM.

The applicability for reinforced thermoplastics has been under investigation using four frp of different fibre and matrix material as well as changing fibre volume content. Experimental studies have been done with off-axis and angle-ply cantilever beam specimens to provoke different shear behaviour (Fig. 1).

The energy related modelling has been implemented for a state of the art FEA software and has been further on used to investigate the energy distribution of the different mode shapes. The study

Table 1 State of the art of elastic and damping properties for different frp using the strain energy dissipation related damping model

fibre	matrix	v_f %	E_1 GPa	E_2 GPa	G_{12} GPa	ν_{12}	Ψ_1 %	Ψ_2 %	Ψ_{12} %	
carbon	epoxy	50	189	6.1	2.7	0.30	0.64	6.90	10.00	(Adams <i>et al.</i> 1973)
carbon	epoxy	50	104	7.6	3.8	0.30	0.49	5.48	10.00	(Adams <i>et al.</i> 1973)
carbon	epoxy	50	173	7.2	3.8	0.29	0.45	4.22	7.05	(Ni <i>et al.</i> 1984)
e-glass	epoxy	50	38	10.9	4.9	0.29	0.87	5.05	6.91	(Ni <i>et al.</i> 1984)
carbon	epoxy	54	113	8.4	4.8	0.30	0.74	7.30	6.60	(Adams <i>et al.</i> 1994)
e-glass	epoxy	54	42	12.5	5.0	0.20	1.61	6.70	7.30	(Adams <i>et al.</i> 1994)
carbon	epoxy	n.a.	125	10.2	6.3	0.34	0.55	4.98	5.92	(Maheri <i>et al.</i> 2003)
carbon	epoxy	61	128	9.2	6.5	0.30	0.42	3.50	4.40	(Maheri <i>et al.</i> 1995)
carbon	epoxy	54	110	9.0	3.9	0.34	0.75	5.95	6.79	(Maheri <i>et al.</i> 1995)
glass	epoxy	n.a.	30	5.9	2.5	0.24	1.51	9.42	12.57	(Li <i>et al.</i> 2014)
carbon	epoxy	n.a.	110	8.6	6.0	0.28	1.13	3.27	5.34	(Li <i>et al.</i> 2013)
graphite	epoxy	n.a.	119	8.7	5.2	0.31	0.74	3.90	0.74	(Li <i>et al.</i> 2013)
e-glass	epoxy	40	30	5.9	2.5	0.24	2.20	8.17	11.31	(Berthelot 2006)
kevlar	epoxy	40	51	4.5	2.1	0.29	9.42	15.71	23.88	(Berthelot 2006)
glass, UD	epoxy	40	30	7.5	2.3	0.24	2.20	8.17	11.31	(El Mahi <i>et al.</i> 2008)
glass, woven	epoxy	40	28	11.0	3.8	0.24	3.14	7.79	10.05	(El Mahi <i>et al.</i> 2008)
glass, taffeta	epoxy	40	14	13.5	2.1	0.25	4.15	4.08	9.42	(El Mahi <i>et al.</i> 2008)
glass, serge	epoxy	40	16	15.4	2.1	0.24	4.21	4.21	9.61	(El Mahi <i>et al.</i> 2008)
carbon	epoxy	n.a.	271	6.0	5.5	0.34	0.45	7.30	8.16	(Maheri <i>et al.</i> 2008)
carbon	PEEK	n.a.	78	6.3	3.9	0.31	0.28	0.94	2.29	(Täger <i>et al.</i> 2015)
carbon	epoxy	n.a.	118	8.1	4.1	0.30	0.47	2.29	2.61	(Täger <i>et al.</i> 2015)
glass	epoxy	n.a.	29	9.4	3.4	0.33	0.88	3.52	4.46	(Täger <i>et al.</i> 2015)
glass	PP	n.a.	17	3.2	1.5	0.31	2.64	13.19	12.82	(Täger <i>et al.</i> 2015)
glass	PA6	n.a.	24	6.3	2.4	0.26	3.39	21.17	21.11	(Täger <i>et al.</i> 2015)
carbon	epoxy	n.a.	156	8.2	4.5	0.34	1.42	1.90	8.10	(Vescovini <i>et al.</i> 2015)

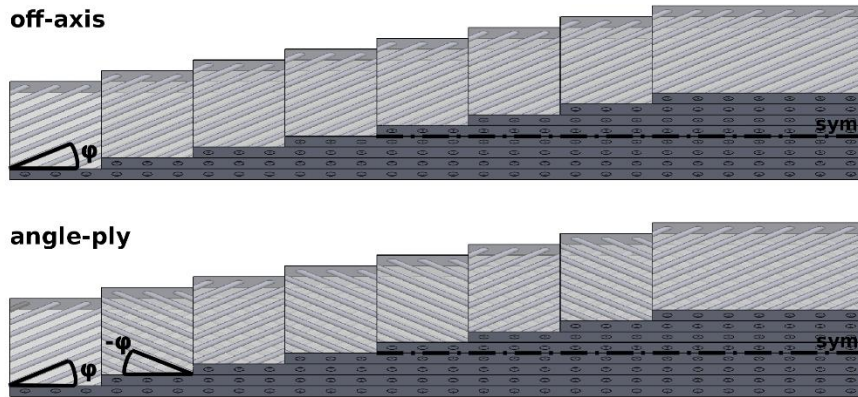


Fig. 1 Symmetric lay-up configurations: off-axis vs. angle-ply beam specimens

implies the experimental setup with cantilever beams and other boundary conditions as well as plates and a curved demonstrator. Finally, the damping model has been applied to determine a velocity based radiated sound power from steady state dynamic simulations.

2. Theoretical background

Laminate properties are usually based on the CLT for orthotropic materials and hence imply perfect bonding between all plies, no strains or stresses out of plane, linear elastic behaviour and small deformations. The notation used here is number subscripts (1, 2, or 12) for the principal material directions of a lamina as well as letter subscripts (x , y , or xy) for the global laminate coordinates. Therein, the normal direction of the thin-walled laminate is equally 3 and z and simultaneously the rotation axis for the transformation of the two coordinate systems with offset angle ϕ .

The described anisotropic damping model assumes the characterisation of the elastic and damping properties of multi-layered composite beams by three basic deformation modes: longitudinal - fibre direction, transverse to the fibre direction and transverse shear deformations (Adams *et al.* 1994). Moreover, it is based on identical elastic behaviour for tension and compression for low stress amplitudes. For practical relevant sufficiently thin laminae, the state of plane stress is assumed in each lamina. Inter-laminar shearing occurs mostly for thick laminae and therefore is neglected here. In addition, common symmetric laminates do not show bending-stretching coupling.

Dissipation within the material can be described by the specific damping capacity (SDC)

$$\psi = \frac{\Delta U}{U} \quad (1)$$

with the total energy dissipated per vibration cycle

$$\Delta U = \frac{1}{2} \int_V \psi \cdot \sigma \cdot \varepsilon \cdot dV \quad (2)$$

including the stress amplitude σ and its corresponding strain amplitudes ε at any point of the material referring to the maximum strain energy U during the vibration cycle. The sum of its separation

$$\Delta U = \Delta U_x + \Delta U_y + \Delta U_{xy} \quad (3)$$

includes components related to different normal stresses in normal (σ_x) and transverse direction (σ_y) as well as the in-plane shear stress (σ_{xy}). The overall laminate damping capacity can be written as (Billups *et al.* 2008)

$$\psi_{laminare} = \psi_x + \psi_y + \psi_{xy}. \quad (4)$$

Historically, the model has been developed for the one-dimensional case first. Hence, for an unidirectional reinforced beam with 0° fibre orientation, there are only longitudinal tension and compression stresses (Adams *et al.* 1973). Based on the dissipation related to σ_x and assuming $\sigma_y = \sigma_{xy} \approx 0$ for free flexure of beams

$$\Delta U_x = \frac{1}{2} \int_V \psi_1 \cdot \varepsilon_x \cdot \sigma_x \cdot dV. \quad (5)$$

Leading to the specific damping capacity referring to σ_x for a laminate with N layers

$$\psi_x = \frac{4}{3} \frac{h^3}{C_{11}} \frac{\psi_1}{N^3} \sum_{k=1}^N T_{ij\varepsilon}^{-1} C_{ij} Q_{ijk} C_{ij} m_k^2 [k^3 - (k-1)^3] \quad (6)$$

with $i=1, j=1,2,3$, the off-axis plane stress stiffness matrix of every thin lamina k Q_{ijk} , the flexural compliance of the laminate C_{ij} , the strain transformation matrix according to CLT $T_{ij\varepsilon}$ and the orientation of every k -th layer $m_k = \cos\phi_k$ or $n_k = \sin\phi_k$.

The ABM requires three material specific damping coefficients for each lamina k : the longitudinal (fibre direction) coefficient ψ_{1k} , the transverse coefficient ψ_{2k} as well as the in-plane shear coefficient ψ_{12k} .

With respect to bending-twisting coupling for free flexure (Ni *et al.* 1984) and neglecting the transverse strain ε_y , this finally leads to the expressions for the different dissipation modes

$$\psi_x = \frac{4}{3} \frac{h^3}{C_{11}} \frac{\psi_1}{N^3} \sum_{k=1}^N \left\{ m_k^2 (m_k^2 C_{11} + n_k^2 C_{12} + m_k n_k C_{16}) \cdot (C_{11} Q_{11k} + C_{12} Q_{12k} + C_{16} Q_{16k}) [k^3 - (k-1)^3] \right\} \quad (7)$$

$$\psi_y = \frac{4}{3} \frac{h^3}{C_{11}} \frac{\psi_2}{N^3} \sum_{k=1}^N \left\{ n_k^2 (n_k^2 C_{11} + m_k^2 C_{12} + m_k n_k C_{16}) \cdot (C_{11} Q_{11k} + C_{12} Q_{12k} + C_{16} Q_{16k}) [k^3 - (k-1)^3] \right\} \quad (8)$$

$$\psi_{xy} = \frac{4}{3} \frac{h^3}{C_{11}} \frac{\psi_{12}}{N^3} \sum_{k=1}^N \left\{ m_k n_k (2m_k n_k C_{11} - 2m_k n_k C_{12} - (m_k^2 - n_k^2) C_{16}) \cdot (C_{11} Q_{11k} + C_{12} Q_{12k} + C_{16} Q_{16k}) [k^3 - (k-1)^3] \right\} \quad (9)$$

assuming N layers of equal thickness and material but only different orientation. It should be mentioned that the original formulations are based on symmetric laminates with an even number of plies and are rewritten here for an arbitrary quantum. Commonly, only symmetric laminates are of practical relevance to avoid mid-plane strains and, thus, distortion in manufacturing. The given but similar equations now allow layups with odd symmetry, too. Further on, only laminates with equal ply materials are discussed. Hence the elastic and dynamic material parameters are not ply specific.

3. Experimental damping determination

There are numerous different methods for experimental damping characterisation with impulse or transient excitation, in frequency or time domain. Commonly, either the loss factor, the damping ratio, the logarithmic decrement or the reverberation time are determined (Petrone *et al.* 2015). Whereas forced vibrational analysis dynamic mechanical analysis (DMA) is limited to low frequencies, modal analysis

In this study, damping has been determined using free vibrations of cantilever beam specimens in the first bending mode with non-contact inductive excitation and non-contact velocity measurement by a laser-doppler-vibrometer.

3.1 Free vibrations of cantilever beams

Assuming free damped vibrations of cantilever beams, the natural frequencies are given by (Dresig *et al.* 2010, Magnus *et al.* 1995)

$$\omega_i = \lambda_i^2 \sqrt{\frac{EH^2}{12\rho L^4}} = 2\pi f_i \quad (10)$$

with the E and ρ respectively Young modulus and density of the material, L length of the beam and H height of the rectangular cross section. Hence, ω is not depending from the beam width.

The solutions λ_i of the frequency equation of cantilever beams

$$1 + \cos \lambda \cdot \cosh \lambda = 0 \quad \text{with} \quad \lambda_1 \approx 1.8752 \quad (11)$$

give the coefficients for the natural frequencies. Related to the experimental setup, measurements have been strictly focussed on only the first bending mode of the cantilever beam. Velocity has been determined at a single point on the middle of the free edge of the beam. The sinusoidal excitation has been performed in the first natural frequency until interruption. Finally, a digital low pass filter excludes any higher resonances from the parameter determination. After all, the derived descripton for the time domain results is similar to single degree-of-freedom oscillator.

For viscous damping the decay is described by an exponential envelope function $\pm Ce^{-\delta t}$. The displacement follows a superposition of an exponential decay and a harmonic vibration, starting at the initial elongation u_0 .

$$u(t) = u_0 \cdot e^{-\alpha t} \cdot \cos(\omega t). \quad (12)$$

Moreover, the decay of the velocity follows similarly

Table 2 Elastic properties of all thermoplastic frp in this study

name	fibre	matrix	v_f %	E_1 GPa	E_2 GPa	G_{12} GPa	ν_{12}
Elekon Plytron	glass	PP	35	28.9	3.7	1.1	0.25
Ticona Celstran GF PP 60	glass	PP	34	26.5	4.3	1.3	0.27
Ticona Celstran GF PP 70	glass	PP	44	31.6	4.5	1.4	0.31
Ticona Celstran CF PA 60	carbon	PA6	44	97.0	4.6	1.3	0.25

$$v(t) = -v_0 \cdot e^{-\delta t} \cdot \sin(\omega t) = -u_0 \cdot \omega \cdot e^{-\delta t} \cdot \sin(\omega t). \quad (13)$$

Considering the whole decay period of the damping behaviour and, thus, neglecting amplitude effects, the damping ratio is given by

$$\psi = \frac{\delta}{\omega_1} \quad (14)$$

as another dimensionless damping parameter the logarithmic decrement is the ratio of two following elongation maxima

$$\Lambda = \ln \left(\frac{\hat{x}_n}{\hat{x}_{n+1}} \right) = \frac{1}{m} \ln \left(\frac{\hat{x}_n}{\hat{x}_{n+m}} \right). \quad (15)$$

3.2 Materials and specimens

For the investigations four different thermoplastic frp with unidirectional plies have been used. The study includes two glass-polypropylene (PP) materials of similar fibre fraction (35%) and different manufacturers, one more glass fibre reinforced PP with 44% fibre fraction as well as a carbon fibre reinforced polyamide 6 (PA6). The detailed elastic material parameters have been determined by quasi-static tensile test according to DIN EN ISO 527 and DIN EN ISO 14129 and are summarised in Table 2.

The tapes had been pre-impregnated either by melt or by a foil with a ply thickness between 0.15 and 0.25 mm. For comparability, approximately 2 mm thick plates with 8 or 12 layers have been produced by a one-step pressing with variable temperature.

Two different set-ups of specimens with orientations between 0° and 90° and a step size of 15° have been prepared. Namely, there were *off-axis* layups with all layers in ϕ -direction as well as symmetric and balanced *angle-ply* laminates with a $[\phi, -\phi]_{ns}$ stacking, meaning n-times repeated sets with layers of positive and negative orientation with similar angle (Fig. 1).

The beam specimens were of nominal dimensions 200 mm×15 mm×2 mm and, hence, a free vibration length of 180 mm. For all layups and orientations 3-5 specimens were tested.

3.3 Experimental setup

Damping of thermoplastic frp has been measured based on the free decay of a cantilever beam. The setup shown in Fig. 2 includes a non-contact out-of plane velocity measurement with a single



Fig. 2 Experimental setup for free vibrations of cantilever beams: laser doppler vibrometer (1), cantilever beam specimen (2), clamping with force monitoring (3) and a harpin coil for inductive excitation (4)

point laser doppler vibrometer (1), the beam specimen vibrating in horizontal direction (2), a clamping with force monitoring (3) to assure constant normal forces below the material strength and a harpin coil for non-contact inductive excitation (4). In addition, a 0.05 mm thin steel sheet has been attached to the plastic specimens at the end. This anchor mass is of negligible stiffness and attached at a beam section with low deformations. Besides, the additional mass is less than 1.5 % of the specimen weight. Hence, the influence of the steel anchor is neglected both in experiments and simulations.

For a direct damping determination in time domain by the exponential decay curve given by Eq. (13), only one vibration mode of the time signal is permissible. Therefore, the cantilever beam is excited harmonically in its first natural frequency f_1 . After interrupting the excitation, the velocity of the decay curve is measured.

The analogue velocity signal is digitalised by a National Instruments PXI-5922 converter and later interpreted by a LabView code. Therein, a low pass filter at πf_1 minimizes additional noise of higher modes. Further on, the damping ratio has been determined in time domain. First, the extraction of the local maxima within the velocity decay curve was used for the identification of the parameters of the exponential envelope function. In addition, the period and, thus, the angular natural frequency was used to determine the damping ratio according to Eq. (14).

All tests were carried out at room temperature (22°C) in air.

3.4 Damping results for thermoplastic composites

Fig. 3 shows the achieved results for all investigated composite materials and therein the expected dependency on the fibre orientation. All glass fibre reinforced thermoplastics show a very similar behaviour with a specific damping capacity up to approximately 10 %. Besides, carbon-PA6 achieves higher damping probably based on the different matrix material but only little on the stiff reinforcing. In general, all off-axis curves peak in a wide range between 30° and 90°. Angle-ply specimens differ significantly to smaller values at 15°-30° and slightly outreach the unidirectional damping in mid and higher angles.

3.5 Numerical determination of damping coefficients

The mean values of the damping for each layup have been analysed considering the ADAMS-BACON criterion described by Eqs. (7) to (9) neglecting the contributions due to the lateral strain (Ni *et al.* 1984). Therefore, the anisotropic damping coefficients have been determined by a curve fitting considering the elastic parameters of Table 2 with an iterative NELDER-MEAD simplex method in Matlab (Mathworks 2013). The results have been constrained to a feasible domain [0...1].

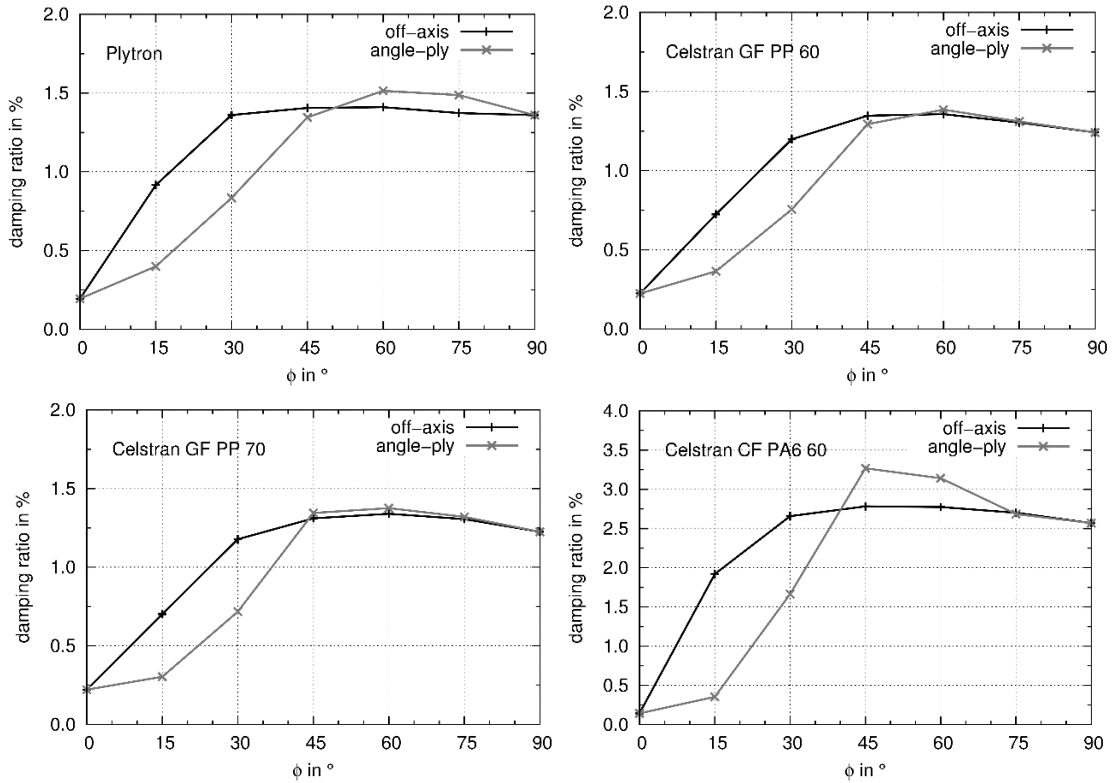


Fig. 3 Specific damping capacity ψ of four thermoplastic composite materials: off-axis vs. angle-ply results

The parameter identification has been done separately for off-axis and angle-ply layouts. In general, the ADAMS-BACON model shows a good correlation to the test results (Fig. 4).

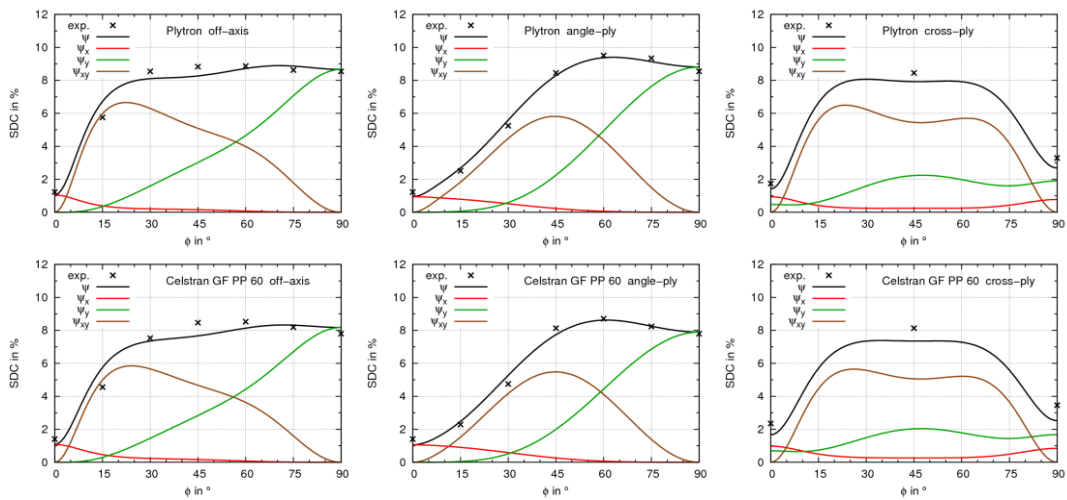


Fig. 4 Specific damping capacity of all thermoplastic composites: test results vs. ADAMS-BACON model

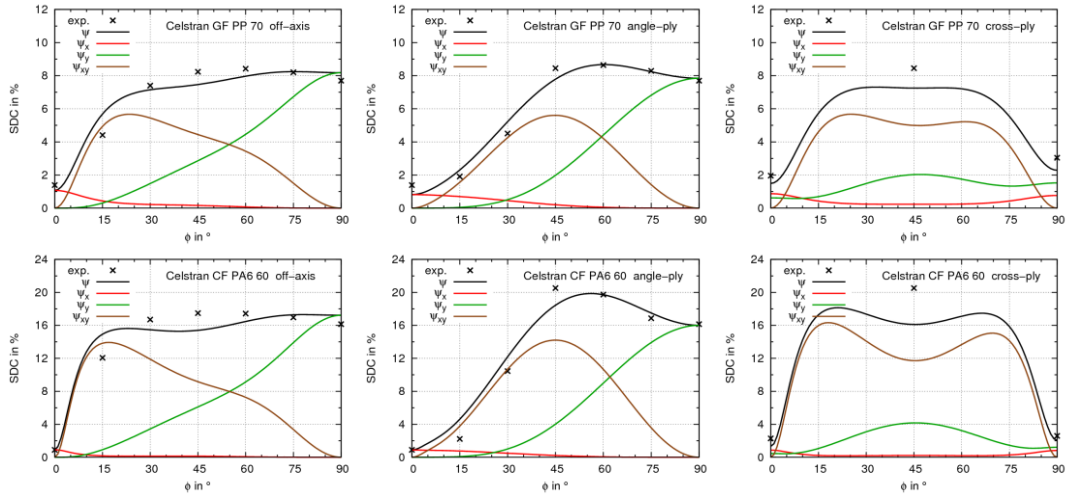


Fig. 4 Continued

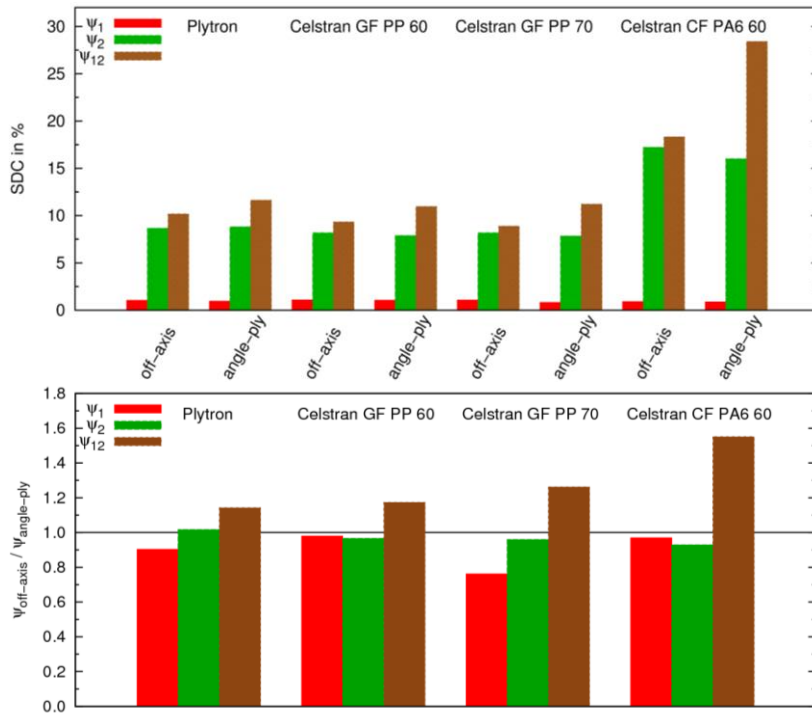


Fig. 5 Comparison of SDC coefficients due to the ADAMS-BACON model: absolute values and relation of off-axis and angle-ply results

The determined coefficients of SDC are compared in Fig. 5 and Table 3. The longitudinal and transverse damping ψ_1 and ψ_2 has been identified in both cases with a good accuracy compared to the 0° and 90° test results which correspond direct to the ABM-coefficients. In contrast, the shear damping has been determined 15% to 50% higher for angle-ply test results than for off-axis

Table 3 Summary of determined SDC coefficients of thermoplastic composites referring to the ADAMS-BACON model

	off-axis			angle-ply		
	Ψ_1 %	Ψ_2 %	Ψ_{12} %	Ψ_1 %	Ψ_2 %	Ψ_{12} %
Elekon Plytron	1.04	8.66	10.18	0.94	8.81	11.63
Ticona Celstran GF PP 60	1.08	8.17	9.34	1.06	7.90	10.96
Ticona Celstran GF PP 70	1.07	8.18	8.89	0.82	7.85	11.21
Ticona Celstran CF PA 60	0.91	17.22	18.32	0.88	16.00	28.41

values. This indicates interlaminar shear deformations and hence the limits of the assumptions of CLT and ABM.

In comparison to published results with epoxy based frp (Table 1) all damping contributions of the PP based composites are similar. In contrast, carbon fibre reinforced PA6 shows up to one time bigger dissipation behaviour. This is caused by a higher damping capability of the PA6 rather than PP in combination with significantly higher losses at the fibre-matrix interface due to the stiffness gradient between carbon fibre and thermoplastics.

In addition, the applicability of the model has been secured by cross-ply laminates with specimens in 0°, 45° and 90° direction using the average of angle-ply and off-axis damping coefficients in Table 3. Thus, the ABM slightly underestimates the damping of the specific layup (Fig. 5). Again, the reason is assumed to be interlaminar shear as the stacking includes numerous angular changes between the plies.

It should be mentioned, that including the contributions of the lateral strains as in Adams *et al.* (1994) gives even better correlation for the off-axis results. Nevertheless, this has been neglected due to questionable results according to negative ψ_y for small non-negative angles in angle-ply laminae of all composite materials in literature and current tests (Billups *et al.* 2008).

4. FEA implementation

For standard FEA codes, there is not any known model describing anisotropic or at least orthotropic material damping. A reasonable option of considering damping of frp is either a viscous damping of a complex stiffness assumption. Both options are usually limited to only one single coefficient (per mode) assuming isotropic material behaviour. A method of synthesized composite damping based on micromechanics implemented by the common Rayleigh-damping approach has been introduced by Kaliske *et al.* (1995).

Owing to the fact, that damping in orthotropic materials is a combination of both material properties and modal deformation characteristics, the implementation is based on mode shapes using the deformation energies of the single modes for the determination of individual assigned modal damping coefficients.

Thus, the mode shapes are analysed with respect to their strain energy components resulting in energy weighted damping coefficients for the different modes. The estimates are given for the three-dimensional stress state. Therefore, the direction are now double indexed instead of using single numbers for the normal stresses before.

In detail, the damping of a single mode

$$\begin{aligned}\psi_{tot} &= \frac{\psi_{11}U_{11} + \psi_{22}U_{22} + \psi_{33}U_{33} + \psi_{12}U_{12} + \psi_{13}U_{13} + \psi_{23}U_{23}}{U_{11} + U_{22} + U_{33} + U_{12} + U_{13} + U_{23}} \\ &= \frac{\sum_{i=1}^3 \sum_{j=i}^3 \psi_{ij} U_{ij}}{\sum_{i=1}^3 \sum_{j=i}^3 U_{ij}}\end{aligned}\quad (16)$$

consists of weighted dissipation energy components related to the sum of these separable strain energies. For the plain strain condition i and j are limited to $[1, 2]$. The strain energy of a single layer k in fibre coordinates

$$U_{ijk} = \frac{1}{2} \int \sigma_{ijk} \varepsilon_{ijk} dV_k \quad \text{for } k = 1 \dots N \text{ and } i, j = 1 \dots 3 \quad (17)$$

leads to the energy sum of the whole model for a single mode shape

$$U_{ij} = \sum_{\text{elements}} \sum_k^N U_{ij k}. \quad (18)$$

In addition, a relative modal strain energy will be used to characterise the contributions of the separable energy components and hence the related damping

$$U_{rel_{ij}} = \frac{U_{ij}}{U_{tot}} = \frac{U_{ij}}{\sum_{i=1}^3 \sum_{j=i}^3 U_{ij}}. \quad (19)$$

Comparing Eq. (16) with the given material parameters from the state of the art (e.g., Table 1) and the derived experimental results (e.g., Table 3) only plane stress related damping coefficients are shown. There is a lack of all damping coefficients related to the 3-direction, though.

Due to the transversal orthotropic behaviour of unidirectional fibre reinforced composite plies, the additional damping coefficients can be derived coefficients from the state of plane stress similarly to the assumptions of static stiffness within the classical laminate theory

$$\psi_{13} = \psi_{12}, \quad \psi_{33} = \psi_{22}. \quad (20)$$

In contrast, the shear deformations in 23-direction are insignificant (Lin *et al.* 1984). Nevertheless, the coefficient for intralaminar shear will be used here as

$$\psi_{23} = \psi_{12}. \quad (21)$$

The modal damping determination has been implemented as user defined post processing algorithm of the numerical modal analysis. Further on, the damping coefficients have been used to investigate different boundary conditions of material testing scenarios and a sound power estimation of a thin-walled frp-structure.

5. FEA-based parametric studies and determination of the sound radiation

The derived strain energy dissipation based modal damping implementation has been further on used to determine the damping of beams and plates with different boundary conditions. As a sample of application the sound radiation of a complex thin-walled frp part has been identified.

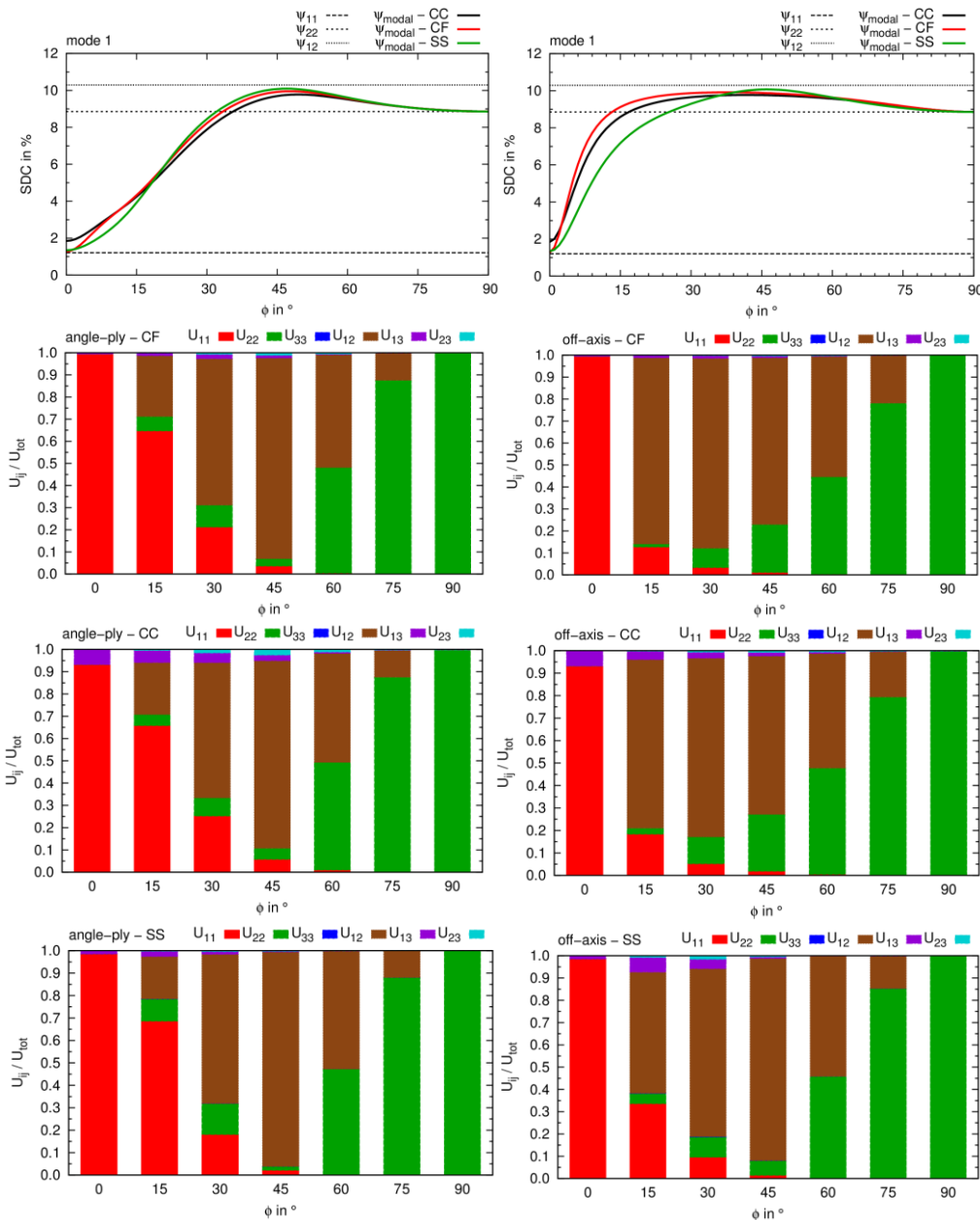


Fig. 6 Damping values for the first bending mode of off-axis (left) and angle-ply (right) beams and relative strain energy distribution of the separable components

All case studies were carried out with glass-fibre reinforced polypropylene (Plytron). In spite of the different damping parameters determined for angle-ply and off-axis layups, the mean value of both contrary results has been used for the SDC.

5.1 Beam specimens with different boundary conditions

Similar to the experiments in section 3, the beam specimens of equal geometry and material have been under investigation for the energy based numerical damping estimation. The model consists of app. 20,000 nodes and 2,700 quadratic solid elements with a layer based stiffness definition. The mode shapes have been determined with three different sets of boundary conditions-clamped/free for the cantilever beam (CF), both edges clamped (CC) as well as both edges simply supported (SS). A parametric study has been done using the layup definitions analogous to the experiments: angle-ply and cross-ply layups between 0° and 90° with a step size of 15° .

Significant deviations between 15° and 45° for the derived damping coefficients under different boundary conditions are shown in Fig. 6. The model portrays the general damping characteristics of angle-ply and off-axis layups known from the literature and measurement results. In contrast to the cantilever beam, two-sided clamped or simply supported setups show significant transverse shear energy in 13-direction up to 45° . This reaffirms the suitability of the chosen boundary conditions for the damping determination. As expected, the 23-component is almost negligible whereas the 33-component is absent in all cases due to the stiff behaviour in thickness direction.

5.2 Squared plate with different boundary conditions

In addition, the parametric study has been extended to a unidirectional reinforced plate of $260 \times 260 \times 2$ mm with three different boundary conditions: all edges free (FFFF), clamped (CCCC) or simply supported (SSSS). The FEA model with element size of 1 mm and one element over thickness consists of approximately 120,000 nodes and 17,000 quadratic layered solid elements.

The FFFF-case underlines the validity of the energy related damping model (Fig. 7). The first mode (1,1) is almost entirely attributed to torsion-only 3% of longitudinal damping are certifiable. Similarly, the second (1,0) and fourth (2,0) mode are purely connected to transversal damping. In

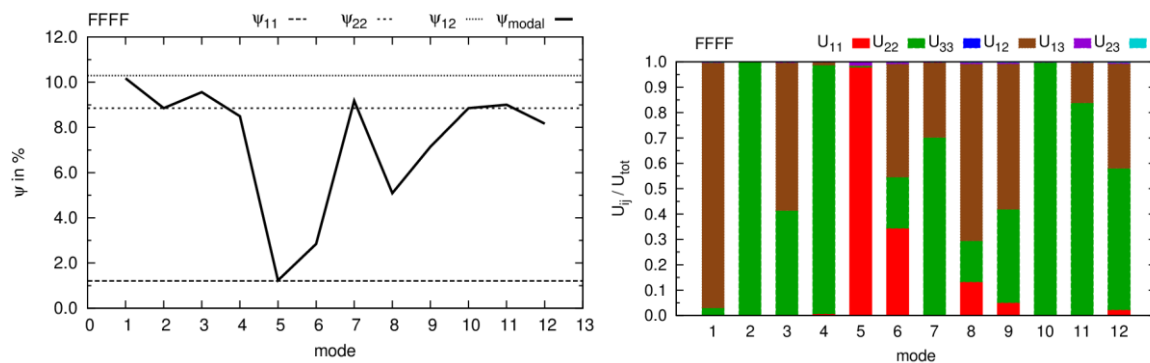


Fig. 7 Modal specific damping capacity and relative strain energy distribution of the separable components of a squared unidirectional reinforced frp plate with free-free boundary conditions

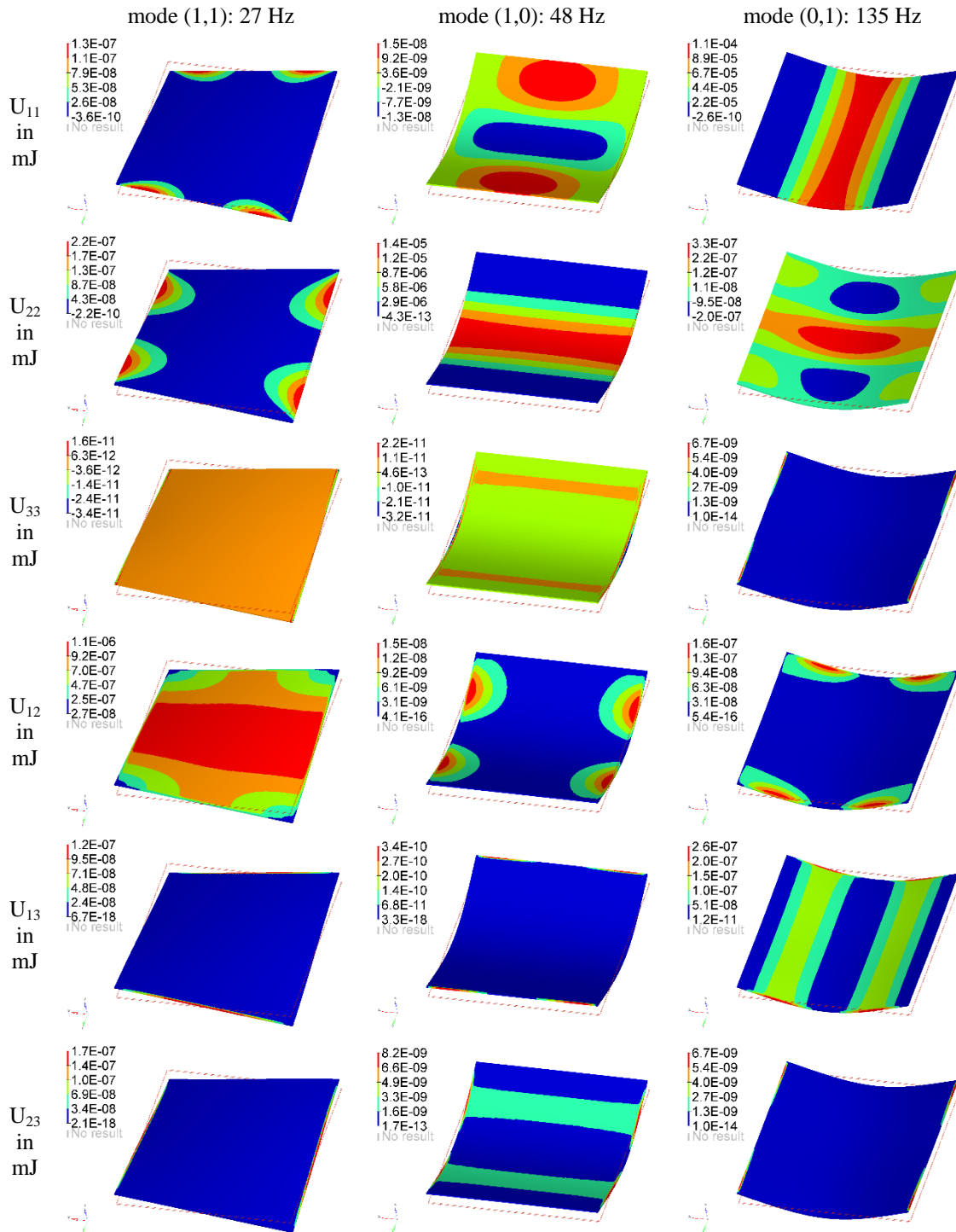


Fig. 8 Mode shapes (1,1), (1,0) and (0,1) of a squared unidirectional reinforced frp plate with all free boundary conditions and strain energy distributions (sum of all layers per element) dominated by shear, transversal and longitudinal damping

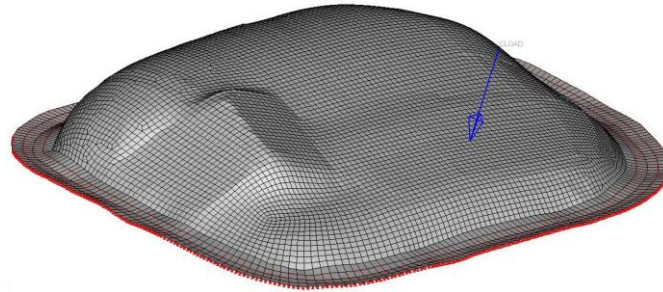


Fig. 9 Demonstrator part: pan with clamped boundary conditions and a point force excitation

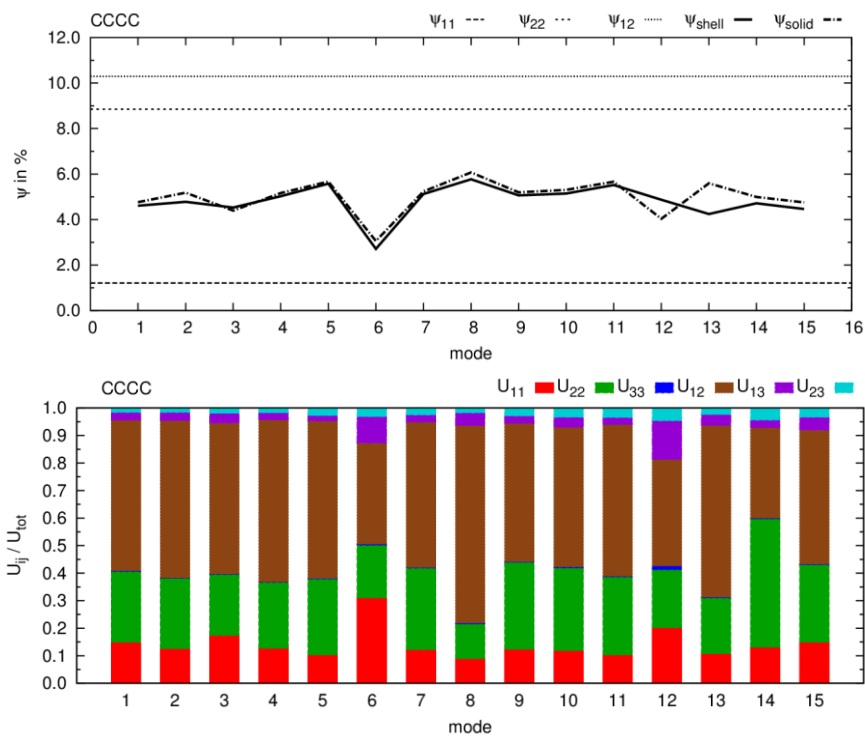


Fig. 10 Modal specific damping capacity and relative strain energy distribution of the separable components of a thin-walled pan with clamped boundary conditions

contrast, the fifth mode (0,1) represents the longitudinal bending in fibre direction. Fig. 8 outlines additionally the local strain energy distributions of all six components. Subsidiary shares of the discussed modes are basically due to edge effects.

In contrast, damping of the SSSS-plate does not exceed the ψ_{22} value but varies between 1% and 9%. It should be mentioned that all modes come with at least two but mainly all three different major energy contributions of the state of plane strain. Transversal shear damping is generally negligible. Thus, none of the damping constants could be determined straight from a single mode.

The specific damping capacity of the all sided clamped bedding is of similar variation and is again commonly a mixture of the three plain stress contributions. Opposed to the simply supported

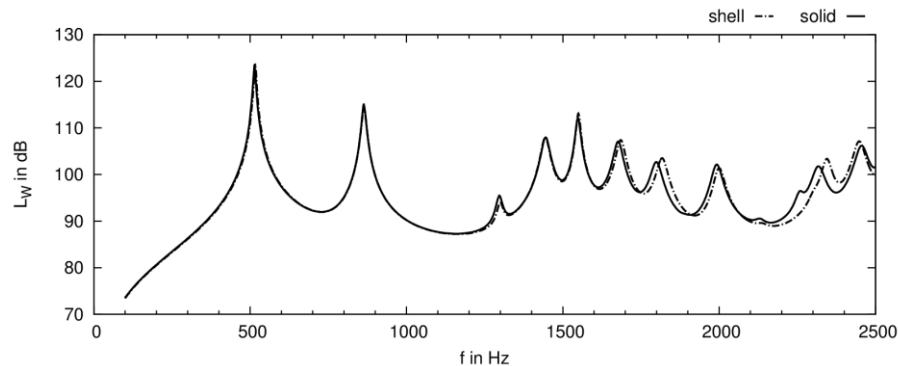


Fig. 11 Radiated sound power of a thin-walled pan with clamped boundary conditions and point force excitation: shell vs. solid model

case, transversal shear component 13 is present with 1% to 15% in all modes.

In summary, the FFFF case is of practical interest for material testing and isolated distortion conditions. It is commonly used to eliminate effects of boundary conditions of the measurements, especially for numerical validations. However, for mounted structures with joints the CCCC indicates the most realistic assembly condition and includes essential transversal shear.

5.3 Sound radiation of a thin-walled frp structure

As an industrial application, a thin-walled formed structure of the same material has been analysed. The outer dimensions of the pan shape shown in Fig. 9 are app. 250×210×100 mm. The part is fixed with displacement boundary conditions along the lower edge (red) and excited by a single point load normal to the top surface. Wall thickness is again 2.0 mm whereas the layup has been changed to a 4:1 cross ply stacking with $[0/0/90/0/0]^\circ$, fibre orientation and a layer thickness of 0.2 mm, i.e. ten layers. The laminate is oriented along the longitudinal side of the pan. Again, the mesh has been developed with quadratic elements of approximately 2.5 mm edge length. Thus, the model consists of about 8,500 elements and 17,000 nodes.

Up to 2.5 kHz, 15 modes have been determined with a specific modal damping varying between 3% and 6% (Fig. 10). Therein, transversal shear contributes in all modes at least 5% of the total strain energy and, thus, is not negligible as already shown for the clamped plate. As a result, there are minor deviations of shell and solid based damping modelling for this part whereas the shell model usually underestimates the damping.

A major application of the derived damping results is e.g., an acoustic evaluation of the components. In this case, mode based steady state dynamic FEA of the pan assuming a point force excitation were used to determine the surface velocities. Based on that, the equivalent radiated sound power (Fritze *et al.* 2009, Klaerner *et al.* 2013) can be used to quantify the sound emission of the radiating component (Fig. 11). Therein, the modal damping is of importance especially close to the resonances and hence the frequency bands with significant sound power levels. For the lower frequency range, both shell and solid modelling can be applied with almost similar accuracy. Above 1.5 kHz, modes shift in frequency and slightly in damping. Thus, the solid model is preferable for higher frequencies.

5. Conclusions

The ply based damping definition of anisotropic fibre reinforced plastics by the ADAMS-BACON model has been successfully applied for different thermoset frp in the past. Within this study, the applicability of the ABM for thermoplastic composites offering reduced matrix stiffness has been proven. Minor deviations are shown in comparison of angle-ply and off-axis laminates for all tested composite materials. Essential interlaminar shear deformations conflicting the assumptions both of classical laminate theory and ABM are reasonably assumed to cause this phenomenon. In general, the ABM indicates the major influence of the fibre orientation on the damping characteristics of frp quite well. The method has been successfully validated with cross-ply laminates of all tested materials.

The energy based modal damping implementation in standard FEA software enables the consideration of anisotropic damping in steady state dynamic simulations. Related to the energy distribution, the boundary conditions may enhance the influence of intralaminar shear and, hence, eliminate the validity of a plain stress shell modelling. Nevertheless, cantilever beams and plates with all free edges can be used for material testing with a good accuracy. Last, the impact on the sound radiation can be recognised starting in the mid frequency range.

In summary, the presented method allows the numerical prediction of the sound and vibration characteristics of composite materials which can significantly differ even if there are similar static properties (Sargianis *et al.* 2013).

Acknowledgments

The paper arose in the context of the project DFG-KR 1713/18-1 ‘Schallabstrahlung bei nichtlinearem und lokal variierendem Dämpfungsverhalten von Mehrlagenverbunden’ funded by the Deutsche Forschungsgemeinschaft (DFG) which is gratefully acknowledged.

References

- Adams, R.D. and Bacon, D.G.C. (1973), “Effect of fibre orientation and laminate geometry on the dynamic properties of cfrp”, *J. Compos. Mater.*, **7**, 402-428.
- Adams, R.D. and Maheri, M.R. (1994), “Dynamic flexural properties of anisotropic fibrous composite beams”, *Compos. Sci. Tech.*, **50**(4), 497-514.
- Adams, R.D. and Maheri, M.R. (2003), “Damping in advanced polymer-matrix composites”, *J. Alloy. Compound.*, **355**(1-2), 126-130.
- Adams, R.D. and Singh, M.M. (1996), “The dynamic properties of fibre-reinforced polymers exposed to hot, wet conditions”, *Compos. Sci. Tech.*, **56**(8), 977-997.
- Berthelot, J.M. (2006), “Damping analysis of laminated beams and plates using the ritz method”, *Compos. Struct.*, **74**(2), 186-201, 2006.
- Billups, E.K. and Cavalli, M.N. (2008), “2d damping predictions of fiber composite plates: Layup effects”, *Compos. Sci. Tech.*, **68**(3-4), 727-733.
- Chandra, R., Singh, S.P. and Gupta, K. (1999), “Damping studies in fiber-reinforced composites - a review”, *Compos. Struct.*, **46**(1), 41-51.
- Dresig, H. and Holzweißig, F. (2010), *Dynamics of Machinery: Theory and Applications*, Springer Science & Business Media, Berlin Heidelberg, Germany.

- El Mahi, A., Assarar, M., Sefrani, Y. and Berthelot, J.M. (2008), "Damping analysis of orthotropic composite materials and laminates", *Compos. Part B: Eng.*, **39**(7-8), 1069-1076.
- Fritze, D. and Marburg, S. and Hardtke, H.J. (2009), "Estimation of radiated sound power: a case study on common approximation methods", *Acta Acustica United with Acustica*, **95**, 833-842
- Hazrati Niyari, A. (2013), "Nonlinear finite element modelling investigation of flexural damping behavior of triple core composite sandwich panels", *Mater. Des.*, **46**, 842-848.
- Kaliske, M. and Rothert, H. (1995), "Damping characterization of unidirectional fibre reinforced polymer composites", *Compos. Eng.*, **5**(5), 551-567.
- Kishi, H., Kuwata M., Matsuda, S., Asami, T. and Murakami, A. (2004), "Damping properties of thermoplastic-elastomer interleaved carbon fiber-reinforced epoxy composites", *Compos. Sci. Tech.*, **64**(16), 2517-2523.
- Klaerner, M., Marburg, S. and Kroll, L. (2013), "Simulative measures for structure borne sound radiation of composites", *Proceedings of Meetings on Acoustics - ICA 2013*, Montreal.
- Li, J. and Narita, Y. (2013), "Analysis and optimal design for the damping property of laminated viscoelastic plates under general edge conditions", *Compos. Part B: Eng.*, **45**(1), 972-980.
- Li, J. and Narita, Y. (2014), "The effect of aspect ratios and edge conditions on the optimal damping design of thin soft core sandwich plates and beams", *J. Vib. Control*, **20**(2), 266-279.
- Lin, D.X., NI, R.G. and Adams, R.D. (1984), "Prediction and measurement of the vibrational damping parameters of carbon and glass fibre-reinforced plastics plates", *J. Compos. Mater.*, **18**(2), 132-152.
- Magnus, K., Popp, K. and Sextro, W. (1995), *Schwingungen : Physikalische Grundlagen und mathematische Behandlung von Schwingungen*, Springer-Verlag, Berlin Heidelberg, New York, Germany/USA.
- Maheri, M.R. (2011), "The effect of layup and boundary conditions on the modal damping of FRP composite panels", *J. Compos. Mater.*, **45**(13), 1411-1422.
- Maheri, M.R. and Adams, R.D. (1995), "Finite-element prediction of modal response of damped layered composite panels", *Compos. Sci. Tech.*, **55**(1), 13-23.
- Maheri, M.R. and Adams, R.D. (2003), "Modal vibration damping of anisotropic frp laminates using the Rayleigh-Ritz energy minimization scheme", *J. Sound Vib.*, **259**(1), 17-29.
- Maheri, M.R., Adams, R.D. and Gaitonde, J.M. (1996), "The effect of temperature on the dynamic characteristics of heat-resistant thermoplastic composites", *Compos. Sci. Tech.*, **56**(12), 1425-1434.
- Maheri, M.R., Adams, R.D. and Hugon, J. (2008), "Vibration damping in sandwich panels", *J. Mater. Sci.*, **43**(20), 6604-6618.
- Mathworks Company (2013), MATLAB User Guide - System Identification Toolbox, USA
- Nagasankar, P., Balasivanandha Prabu, S. and Velmurugan, R. (2014), "The effect of the strand diameter on the damping characteristics of fiber reinforced polymer matrix composites: Theoretical and experimental study", *Int. J. Mech. Sci.*, **89**(0), 279 - 288.
- Ni, R.G. and Adams, R.D. (1984), "The damping and dynamic moduli of symmetric laminated composite beams-theoretical and experimental results", *J. Compos. Mater.*, **18**(2), 104-121.
- Petrone, G., D'Alessandro, V., De Rosa, S. and Franco, F. (2014), "Damping evaluation on eco-friendly sandwich panels through reverberation time (RT60) measurements", *J. Vib. Control*, 1077546314522507.
- Sargianis, J., Kim, H., Andres, E. and Suhr, J. (2013), "Sound and vibration damping characteristics in natural material based sandwich composites", *Compos. Struct.*, **96**, 538-544.
- Täger, O., Dannemann, M. and Hufenbach, W. (2015), "Analytical study of the structural-dynamics and sound radiation of anisotropic multilayered fibre-reinforced composites", *J. Sound Vib.*, **342**, 57-74.
- Täger, O., Kroll, L. and Hufenbach, W. (2004), "Vibro-acoustic design of composites", *Kunststoffe Plast Europe*, **94**(11), 118-121.
- Treviso, A., Van Genechten, B., Mundo, D. and Turnour M. (2015), "Damping in composite materials: Properties and models", *Compos. Part B: Eng.*, **78**, 144-152.
- Vescovini, R. and Bisagni, C. (2015), "A procedure for the evaluation of damping effects in composite laminated structures", *Progress in Aerospace Sciences*, <http://dx.doi.org/10.1016/j.paerosci.2015.05.004>.
- Yim, J.H., Cho, S.Y., Seo, Y.J. and Jang, B.Z. (2003), "A study on material damping of 0° laminated composite sandwich cantilever beams with a viscoelastic layer", *Compos. Struct.*, **60**(4), 367-374.